Microfluidic transport based on direct electrowetting

Wataru SatohMichael LoughranHiroaki Suzuki

Citation: Journal of Applied Physics **96**, 835 (2004); doi: 10.1063/1.1739528
View online: http://dx.doi.org/10.1063/1.1739528
View Table of Contents: http://aip.scitation.org/toc/jap/96/1
Published by the American Institute of Physics

Microfluidic transport based on direct electrowetting

Wataru Satoh
Institute of Materials Science, University of Tsukuba, Tsukuba, Ibaraki, 305-8573, Japan

Michael Loughran
National Microelectronics Research Centre, Lee Maltings, Prospect Row, Cork, Ireland

Hiroaki Suzuki[a)]
Institute of Materials Science, University of Tsukuba, Tsukuba, Ibaraki, 305-8573, Japan

(Received 18 December 2003; accepted 23 March 2004)

An integrated microfluidic system was fabricated which functions by deliberately manipulating interfacial tension. A distinctive characteristic of our system is the use of an array of adjacent, elongated, working electrodes and protruding polydimethylsiloxane open-flow channels. Microfluidic transport was realized directly on the bare gold electrode surface in the absence of an additional dielectric layer. By changing the potential of the working electrode to a negative potential, a liquid column could be transported from one end of an elongated working electrode to the other end. Transport of the liquid column could be altered without any valves by switching on the adjacent electrode in a given direction. The flow velocity depended on the applied potential, i.e., the velocity could be altered by deliberate manipulation of the electrode potential. In addition, the flow velocity increased as the dimensions of the flow channel decreased. The applied voltage was less than 2 V, and the power consumption was in the order of tens of μW. © *2004 American Institute of Physics.* [DOI: 10.1063/1.1739528]

I. INTRODUCTION

An integrated, on-chip fluid transport system is essential to fabricate a future generation sophisticated lab-on-a-chip. Current research trend requires further reduction of the transported volume. As the entire size of micro-systems and channel dimensions are reduced, surface-to-volume ratio increases. Consequently, the influence of interfacial tension becomes dominant. Generally, the interfacial tension has an adverse effect for many mechanical microfluidic systems, since it generates resistive force. Therefore, the use of interfacial tension provides a natural solution to control microfluidic transport and is becoming an important aspect in the current trend toward miniaturization. With this in mind, we utilized the principle of electrowetting to mobilize a liquid.

The studies on electrocapillary effects by Nakamura enabled various kinds of thermodynamic information to be determined.[1,2] In 1980 Minnema established that the surface tension at a polyethylene–water interface decreases strongly under high voltage.[3] The phenomenon of electrowetting was utilized in 1981 by Beni and co-workers to describe the direct electrical control of surface tension on bare electrodes.[4,5] Whilst the pioneering studies did not generate marked progress in device applications until the middle of 1990s, the phenomenon attracted considerable attention over the last several years.[6] In this respect, microfluidic devices have recently provided the most promising applications and several devices have been reported.[7–11] Microfluidic devices based on electrowetting have several advantages when compared to conventional micropumps and microvalves.[12] For example the structure and function can be made very simple, which facilitates a high level of component integration and realization of a sophisticated system. The reduction of operating voltage and power consumption is also another advantage of microfluidic devices which do not incorporate mechanical pumps and valves.

The operation of many of the more recent microfluidic systems has been based on so-called electrowetting on dielectric.[7,8,10] A droplet is placed between electrodes with hydrophobic insulating layers and a voltage is applied between the electrodes. The use of droplets enables on-chip transport to be realized and facilitates microfluidic mixing. However, a concern with this type of device is a high driving voltage. Moon and co-workers verified how to lower the operating voltage to as low as 15 V. This was achieved by using a fluoropolymer coating on a thin dielectric layer having a very high dielectric constant.[13] However, further reduction of voltage does not seem to be easy. This is because the dielectric layer must be very thin while preventing electron transfer and maintaining a high electric field when a potential is applied.[13]

To overcome the problem, we have developed an integrated on-chip microfluidic system which operates by electrochemically manipulating interfacial tension on a bare electrode which is in direct contact with a solution (direct electrowetting). Unlike the previous studies which use a droplet, we transported a liquid continuously from an injection port, because it is a common approach currently used in microfluidic systems.[14,15] Although current generation caused by redox reactions on the electrode surface might be considered a disadvantage, the much lower operating voltage in the absence of a dielectric layer provides a realistic alter-

[a)]Author to whom all correspondence should be addressed; electronic mail: hsuzuki@ims.tsukuba.ac.jp

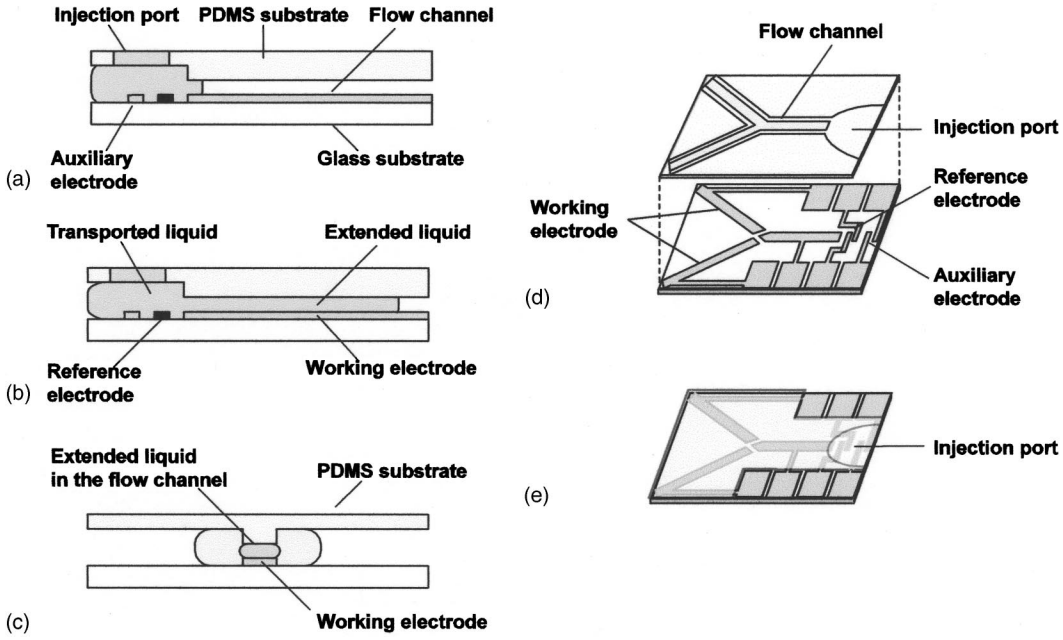

FIG. 1. Construction of the microfluidic system. (a), (b) Cross section to show the basic arrangement of the electrodes and the flow channel, (c) cross section viewed from the right of (a) and (b), (d) decomposed structure of the system, (e) completed system.

native for the future generation lab-on-a-chip devices. When the end of a hydrophilic capillary or planar plates with a narrow gap is immersed in an aqueous solution, the solution rises.[16] The force generated at the advancing meniscus is sufficient to withdraw a solution competing with the gravitational force. This means that the liquid solution can be transported over a much longer distance if the capillary or flow channel is positioned horizontally. Therefore, to enhance the microfluidic transport we utilized an array of elongated working electrodes unlike previous studies which incorporate an array of short working electrodes.[7,10]

To mobilize a liquid using direct wetting, there is a tradeoff between the efficiency of transport and the redox reactions. The latter can be a cause of gas bubble production and increase in power consumption. To control these parameters, the electrode potential must be controlled accurately, which is difficult to achieve with a two-electrode configuration because of the polarization of the counter electrode. Consequently, we utilized a three-electrode system to achieve reproducible and efficient microfluidic transport. The fabrication and characterization of the device is discussed.

II. PRINCIPLE OF OPERATION

When a liquid droplet or column is placed on a polarized metal electrode, the interfacial tension between the electrode and the liquid changes according to the Lippman equation,[17,18]

$$\gamma = \gamma_0 - \tfrac{1}{2} c V^2, \tag{1}$$

where γ is the interfacial tension between the electrode and the liquid, c is the capacitance at the interface per unit area, and V is the voltage of the electrode measured with respect to an appropriate potential standard. The mechanism for force generation in the direction horizontal to the interface has been clarified by other researchers.[19–21] Also, dependence of the performance on physical parameters has been analyzed by Ren and co-workers.[22]

The driving voltage V needed to mobilize a liquid can be approximated as follows:[6]

$$V \approx \sqrt{\frac{\gamma}{C}}, \tag{2}$$

where C is the capacitance at the interface. A voltage of tens or hundreds of volts is often necessary to mobilize a liquid on an insulator, whereas a voltage of 1–2 V is sufficient to mobilize a liquid on a bare electrode. A compromise is that the contact angle change that can be induced is relatively small, which is limited by electron transfer from the electrode to redox active species in the liquid.[13]

Here, it should be emphasized that the voltage expressed under these circumstances should be the one measured with respect to a reliable potential standard with a well-defined potential. This particularly applies to the case in which current is flowing. Therefore, accurate regulation of this voltage requires a pair of electrodes consisting of one polarized driving electrode and a second nonpolarized electrode.[16] Noble metal electrodes such as gold and platinum can be used for the former, whereas a reference electrode such as Ag/AgCl must be used for the latter. Since the potential of the nonpolarized reference electrode is maintained at a constant level, changes in the voltage between the electrodes are almost equivalent to changes in the potential between the polarized electrode and the solution. In such circumstances the voltage is accurately controlled. In practice, a three-electrode configuration should be used, because the consumption of the Ag/AgCl electrode will be rapid in a two-electrode configuration.

The arrangement of electrodes and the principle of operation are shown in Fig. 1. The liquid filled in the injection port first wets the edge of the first working electrode [Fig. 1(a)]. When the potential of the working electrode is changed to an operating value (−0.9 V), the interfacial tension between the electrode and the liquid changes making the electrode more hydrophilic. The advancing meniscus at the front of the column tries to move to establish a new equilibrium. As a result, this change in applied potential facilitated rapid transport of the liquid [Fig. 1(b)].

III. EXPERIMENT

A. Construction of the system

The structure of the system is shown in Fig. 1. The system consists of a glass substrate with driving electrodes bonded to a hydrophobic polydimethylsiloxane (PDMS) substrate with integrated flow channels. Although conventional methods of fabricating microfluidic devices have centered on etching in glass and silicon, fabrication of microfluidic devices in PDMS provides faster, less expensive routes than these conventional methods to devices that handle aqueous solutions.[23]

The driving electrodes consisted of modified three-electrode systems with gold working electrodes, Ag/AgCl reference electrodes, and auxiliary electrodes. The working electrodes were arranged in a single row along the flow channel (see Fig. 2). Two adjacent working electrodes were carefully aligned in such a manner that facilitated wetting of the edge of the next working electrode. The separation between the adjacent electrodes was 200 μm.

The liquid was mobilized along a flow channel defined by a protruding structure in the PDMS substrate, fabricated by casting a PDMS precursor solution on a thick-film photoresist (SU-8) template. In contrast with conventional microfluidic systems, our flow channel had an open structure: the liquid was confined in a space between the ceiling of the protruding channel and the driving electrodes by surface tension. The contact angle of an aqueous solution on PDMS was approximately 100°. Consequently, the solution was confined in the narrow space between the lower and upper substrates [Figs. 1(a)–1(c)]. As for the glass substrate, no protruding structure was necessary and solution transport occurred on the electrode pattern without any problems. However, since the solution in the flow channel exuded to the periphery of the electrode, areas other than the flow channel and the injection reservoir were covered with a hydrophobic negative photoresist (OMR-83) pattern. The width and thickness of the flow channels were 1.0 mm and 50 μm, respectively.

In mobilizing a liquid using direct electrowetting at a low operating potential (~1 V), it is not easy to mobilize the receding meniscus.[10,24] Moreover, the receding meniscus can be a cause of resistive force. Therefore, the novel approach described here utilized a single advancing meniscus at the front of the liquid column and stored as much liquid as possible in a reservoir located at the injection port. In this manner, difficulties associated with the resistive effect of the receding meniscus were minimized.

B. Reagents

The following materials were obtained from commercial sources: negative photoresist (OMR-83, used to passivate the areas other than the flow channel) from Tokyo Ohka Kogyo (Kawasaki, Japan), thick-film photoresist (SU-8) from MicroChem (MA); precursor solution of PDMS (KE-1300T) from Shin-Etsu Chemical (Tokyo, Japan), fluorescein from Wako Pure Chemical Industries (Osaka, Japan), Triton X-100 (surfactant) from Acros Organics, (NJ). All of the other chemicals (reagent grade) were commercially obtained and used without further purification.

C. Procedures

Before using the device, AgCl layer was grown on the silver pattern for the reference electrode by applying 1.0 μA for 1 min in 1.0 M KCl solution (25 °C). The liquid was filled in the injection port from the edge of the substrates by capillary action. In mobilizing the liquid column, the potential of the working electrode was set at −0.9 V (versus on-chip Ag/AgCl) unless indicated otherwise. The potential was set at 0 V when the column was at rest. The column velocity was determined by measuring the time for the column to move from one end to the other end of the first working electrode. A 1.0 M KCl solution was mainly used as a test solution. Fluorescein (10 mM) was added when recording the movement of the liquid column along the flow channel. Fluorescence from the liquid column was recorded with a Keyence VB-6000 fluorescence microscope. All experiments were conducted at room temperature.

IV. RESULT AND DISCUSSION

A. Transport of fluid in flow channels

Once the potential was applied to the working electrode, the motive force generated as a result of the imbalance of interfacial tensions was sufficient to mobilize the liquid column from one end of the electrode to the other [Figs. 2(a) and 2(b)]. Although the ceiling of PDMS exerts a resistive force, a single working electrode at the bottom of the flow channel was sufficient to transport the liquid. When the PDMS substrate was completely flat with no protruding channel structure, the liquid column tended to spread on the PDMS substrate beyond the periphery of the flow channel. The effusion became more significant, and often uncontrolled, especially as the front of the liquid column was mobilized along the flow channel. With the protruding structure, however, the liquid column was effectively confined in a well-defined space between the structure and the working electrode.

In the situation reported here, the front of the liquid column at the Y-channel intersect exuded through a hydrophilic gap area into the edge of the next adjacent working electrode. By switching on the potential of the next working electrode, the liquid column then moved forward in this direction [Fig. 2(c)]. The liquid column did not move to any other electrodes which did not have an applied potential. After the liquid column was transported in a given direction, the column could be split into another direction by applying

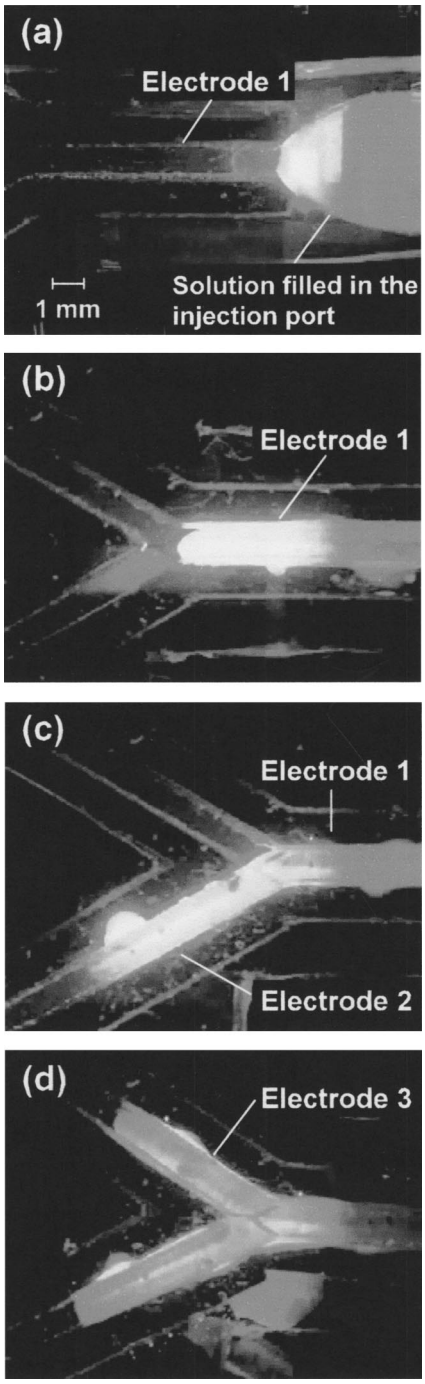

FIG. 2. Transport of liquid through the flow channel. (a) The solution was filled in the injection port. (b) When the potential of electrode 1 was switched on, the solution was mobilized into the flow channel. (c) By switching on the potential of electrode 2, part of the liquid column can then be transported to another flow channel. (d) The column could be split into another direction by applying a potential to electrode 3.

a potential to the working electrode [Fig. 2(d)]. In this manner the liquid column could be moved in a specific direction without any valves.

B. Dependence of the rate of transport on applied potential

The interfacial tension becomes maximum at the point of zero charge (PZC) and decreases monotonically with the increase or decrease in potential from the PZC.[16] The inset to Fig. 3 shows the dependence of the contact angle of a droplet (3 μL) on electrode potential. The maximum was observed around 0 V and the variation of the contact angle was quadratic with respect to V around the PZC. As the contact angle changes due to the applied voltage, surface wettability changes. For example, it may switch between hydrophobic and hydrophilic states. The difference in the contact angle in our research was 35° between 0 and −1.2 V. This observed change in contact angle compares favorably with the previous research of Moon and co-workers,[13] who showed that a 40° contact angle modulation in air can be achieved with applied voltages as low as 15 V.

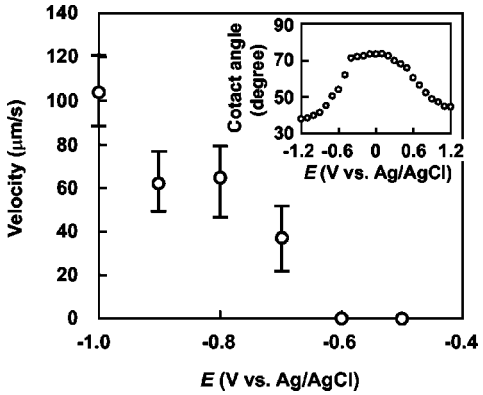

FIG. 3. Dependence of column velocity on applied potential. Five runs were made and the averages and standard deviations are shown. Inset: dependence of contact angle at the advancing meniscus on applied potential.

Figure 3 shows the dependence of the velocity of the liquid column on applied potential. A potential more negative than −0.6 V was necessary to mobilize the liquid. The observed change around this potential was very sharp. The movement of the liquid column became more rapid as the potential became more negative (Fig. 3). Although the velocity becomes higher by making the potential more negative, there is a limitation because the Faradaic current increases and the evolution of hydrogen gas becomes more significant. In cyclic voltammograms taken in the same solution, an increase in current was observed at potentials lower than about −0.8 V. Since it is necessary to reach a practical compromise between the flow velocity and the applied potential, −0.9 V was chosen as a driving potential. The influence of KCl concentration on the transport was small. The increase in flow velocity was 25% when the KCl concentration was increased from 1 mM to 1 M. Therefore, a large change in the ionic strength should not create serious problems.

The configuration of our system is unique compared with many other cases using a droplet in that the meniscus at one end of the liquid column is fixed around the inlet of the reservoir and only the advancing meniscus at the other end is used. A key point which leads to the smooth liquid transport in our system was to store as much liquid as possible in the reservoir to minimize changes in the receding meniscus.

Similar to the model by Kuo *et al.*,[25] when the potential of the driving electrode is changed, the initial column velocity will increase rapidly due to the build up of the internal pressure gradient. This pressure increase is counterbalanced

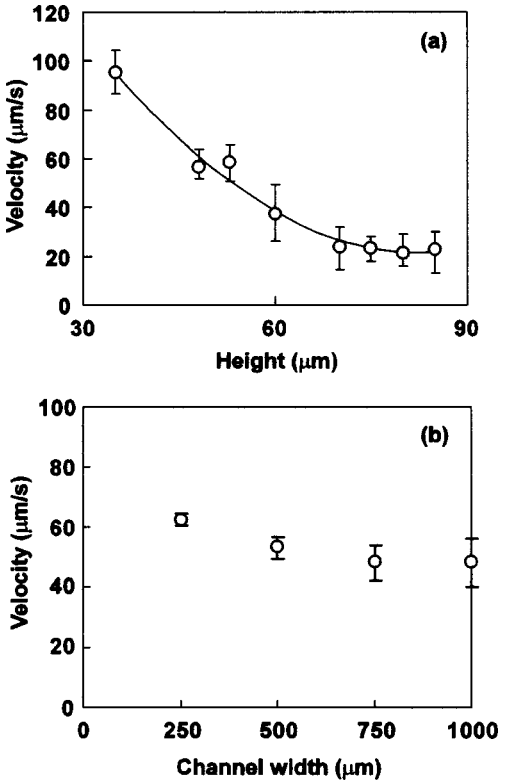

FIG. 4. Influence of the geometry of the flow channel on the fluid transport. (a) Dependence of the column velocity on the height of the flow channel. (b) Dependence of the column velocity on the width of the flow channel (error bars represent standard deviation, $n=5$).

by the viscous resistance, which increases linearly with distance.[25] Actually, it was difficult for the column to reach the ends of the Y-shaped flow channel. Therefore, there might be a limitation on the transported distance on a single long working electrode. However, it will pose no serious problems if the size of the chip is about a centimeter and the electrode patterns are appropriately placed.

C. Dependence of the rate of transport on the geometry of the flow channel

Figure 4 shows the dependence of the velocity of the liquid column on the dimensions of the flow channel. We expected that the liquid column can be transported more effectively at a faster flow velocity as the size of the flow channel decreased since the transported volume is reduced and the driving force is generated only at the menisci at the front of the column. This was actually the case and the flow velocity increased as the gap between the electrode and the ceiling of PDMS was reduced [Fig. 4(a)]. With wider gaps, no dependence was observed. The observed flow velocities measured in our experiment were only micrometers per second. However, we expect that greater velocities can be determined by narrowing the gap of the flow channel. Much higher flow velocities on the order of centimeters per second have been realized by Prins *et al.*, who manipulated the interfacial tension in an alternative configuration.[8]

The variable flow velocity data observed for flow channels wider than 250 μm occurs because uniform transport is more difficult along the entire width of larger flow channels. The insensitivity observed in Fig. 4(b) reflects the fact that driving force generated on the electrode and the resistive force caused by the PDMS ceiling are both exerted in the same direction along the entire length of transported direction.

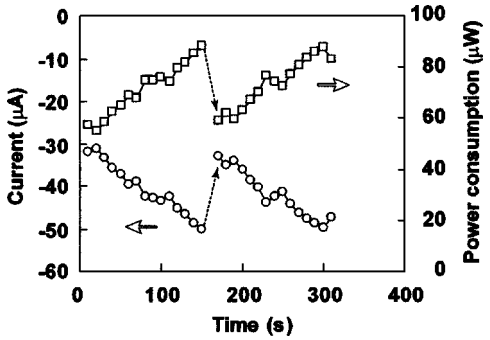

FIG. 5. Variation of current output (○) and power consumption (□) when a liquid column is transported on a working electrode.

D. Current output and power consumption

Figure 5 shows the variation of current and power consumption when a liquid column is transported on two working electrodes. The power consumption was calculated from the generated current and the voltage between the working and auxiliary electrodes. As considered, the current and power consumption increased as the liquid column moved. With the 1.0-mm-wide working electrode, they were on the order of tens of μA and tens of μW, respectively. In this system, the potential of the working electrode can be switched off after the meniscus of the solution wets the edge of the next working electrode: once the liquid has been transported, the first electrode does not generate any effective motive force the origin of which is at the meniscus. Since the contact area on the next working electrode was small at this point, the current and the power consumption dropped to small values. Again, as the column moved on the working electrode, the contact area increased and the current and power consumption increased as with the previous electrode.

Here, a substantial proportion of the current derives mainly from the Faradaic current originating from the reduction of oxygen and proton and the charging current for the double layer. The former varies linearly with the increase in the contact area, whereas the latter changes in proportion to the derivative of the contact area under a constant voltage. In the data shown in Fig. 5, the current is not so small even at the beginning. Since the wetted area on the electrode is limited just after the potential is impressed, the result suggests that the contribution from the Faradaic current is not significant. Therefore, approximately 30 μA of the total current is assumed to originate from the charging current. Note that even the systems with a hydrophobic insulating layer are not free from the charging current, although the Faradaic current might be neglected.[22]

We anticipate that the power consumption could be reduced even further as the size of the microfludic device is reduced. This is because not only the surface area of the

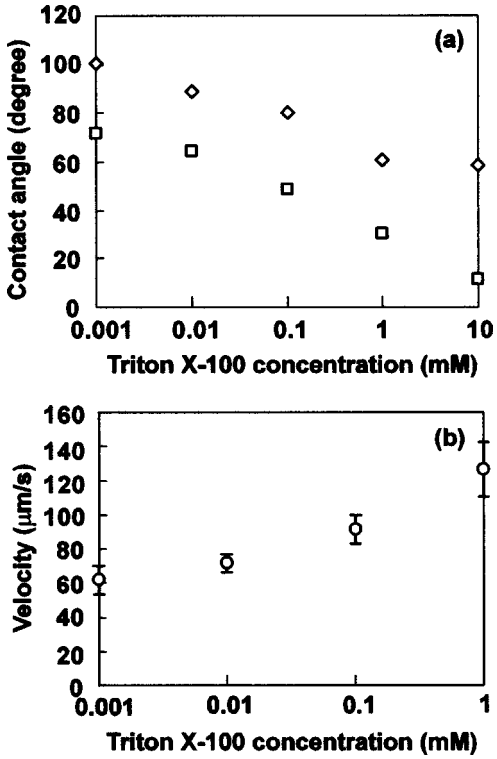

FIG. 6. Influence of surfactant. Dependence of contact angle (a) and dependence of column velocity on the concentration of Triton X-100 (b). In (a), the dependence of wettability on Triton X-100 concentration was compared without impressing potential to the gold thin film. The substrate or underlayer was PDMS (◇) and gold (□).

working electrodes is reduced but also more efficient transport in a narrower flow channel results in a lower operating potential [see Fig. 4(a)]. Furthermore, the use of an almost nonpolarizable electrode (e.g., Ag/AgCl) as the auxiliary electrode will be effective to minimize the power consumption.[26]

E. Effect of surfactant

Rosslee previously reported that surfactants can initiate large and reversible changes in the surface tensions of liquids within seconds.[27] Therefore, it seems logical that microfluidic transport system which utilizes a change in the interfacial tension as a driving force should also consider the influence of surfactants. Here, Triton X-100 was used as a representative surfactant and its influence on microfluidic transport was determined with respect to the dependence of the contact angle on surfactant concentration. A contact angle experiment on a thin-film gold layer (without applying voltage) or the PDMS substrate using 1.0 M KCl containing the surfactant revealed that the adverse effect cannot be avoided [Fig. 6(a)]. For concentrations >10 μM, the experiment revealed monotonic decreases in the contact angle for both cases as the concentration increased. The change was more significant on the gold film than the PDMS substrate suggesting that the former is affected more by the existence of the surfactant. Although the contact angle saturates around 40° without the surfactant (see Fig. 3), it can be much lower than that in the presence of the surfactant.

The influence of Triton X-100 on the transport of liquid was also examined in the system [Fig. 6(b)]. At concentrations >10 μM, the velocity of the liquid column increased as the concentration of the surfactant increased. Although the threshold potential was about -0.6 V without the surfactant, it shifted to about -0.5 and -0.4 V for solutions containing 0.1 and 1.0 mM Triton X-100, respectively. This means that less over-potential is required for the gold electrode and the resistive force at the PDMS ceiling decreases. A small amount of surfactant might have a positive effect in that transport of fluid becomes more efficient. However, at surfactant concentrations >1.0 mM, internal surfaces in the system became too hydrophilic to control fluid transport by changing the electrode potential.

V. CONCLUSIONS

Direct electrowetting enabled the continuous transport of a liquid column through an open flow channel formed between a working electrode and a protruding structure on the PDMS substrate to define the flow channel. Gold working electrodes aligned in a row faced the protruding areas to form flow channels. Switching on the applied potential in sequence, one by one, minimized the current output and power consumption. In this manner the liquid column was transported in a fixed direction. The same electrowetting principle could be utilized to alter the direction of the liquid column at a Y-intersect without using check valves. The mechanism is more effective even as the dimensions of the flow channel decreases, which is a marked contrast to many of the conventional microfluidic systems that incorporate micro pumps and valves.

ACKNOWLEDGMENTS

This study was supported by a Grant-in-Aid for Scientific Research on Priority Areas and by the 21st Century COE Program both under the Ministry of Education, Culture, Sports, Science, and Technology.

[1] Y. Nakamura, K. Kamada, Y. Katoh, and A. Watanabe, J. Colloid Interface Sci. **44**, 517 (1973).
[2] Y. Nakamura, M. Matsumoto, K. Nishizawa, K. Kamada, and A. Watanabe, J. Colloid Interface Sci. **59**, 201 (1977).
[3] L. Minnema, H. A. Barneveld, and P. D. Rinkel, IEEE Trans. Electr. Insul. **15**, 461 (1980).
[4] G. Beni and M. A. Tenan, J. Appl. Phys. **52**, 6011 (1981).
[5] G. Beni and S. Hackwood, Bull. Am. Phys. Soc. **26**, 445 (1981).
[6] C. Quilliet and B. Berge, Curr. Opin. Colloid Interface Sci. **6**, 34 (2001).
[7] M. G. Pollack, R. B. Fair, and A. D. Shenderov, Appl. Phys. Lett. **77**, 1725 (2000).
[8] M. W. J. Prins, W. J. J. Welters, and J. W. Weekamp, Science **291**, 277 (2001).
[9] N. R. Tas, J. W. Berenschot, T. S. J. Lammerink, M. Elwenspoek, and A. van den Berg, Anal. Chem. **74**, 2224 (2002).
[10] J. Lee, H. Moon, J. Fowler, T. Schoellhammer, and C. J. Kim, Sens. Actuators, A **95**, 259 (2002).
[11] K. S. Yun, I. J. Cho, J. U. Bu, C. J. Kim, and E. Yoon, J. Microelectromech. Syst. **11**, 454 (2002).
[12] G. T. A. Kovacs, *Micromachined Transducers Sourcebook* (WCB McGraw-Hill, Boston, 1998), pp. 823–855.
[13] H. Moon, S. K. Cho, R. L. Garrell, and C. J. Kim, J. Appl. Phys. **92**, 4080 (2002).
[14] H. Hisamoto, T. Horiuchi, K. Uchiyama, M. Tokeshi, A. Hibara, and T. Kitamori, Anal. Chem. **73**, 5551 (2001).

[15] M. Tokeshi, T. Minagawa, K. Uchiyama, A. Hibara, K. Sato, H. Hisamoto, and T. Kitamori, Anal. Chem. **74**, 1565 (2002).
[16] J. O. M. Bockris, A. K. N. Reddy, and M. Gamboa-Aldeco, *Modern Electrochemistry*, 2nd ed. (Kluwer Academic/Plenum, New York, 2000), Vol. 2A.
[17] M. Vallet, M. Vallade, and B. Berge, Eur. Phys. J. B **11**, 583 (1999).
[18] H. J. J. Verheijen and M. W. J. Prins, Langmuir **15**, 6616 (1999).
[19] R. Digilov, Langmuir **16**, 6719 (2000).
[20] K. H. Kang, Langmuir **18**, 10318 (2002).
[21] K. H. Kang, I. S. Kang, and C. M. Lee, Langmuir **19**, 5407 (2003).
[22] H. Ren, R. B. Fair, M. G. Pollack, and E. J. Shaughnessy, Sens. Actuators B **87**, 201 (2002).
[23] J. C. McDonald, D. C. Duffy, J. R. Anderson, D. T. Chiu, H. K. Wu, O. J. A. Schueller, and G. M. Whitesides, Electrophoresis **21**, 27 (2000).
[24] W. Satoh and H. Suzuki, in Transducers'03 Digest of Technical Papers, Boston, 2003, pp. 706–709.
[25] J. S. Kuo, P. Spicar-Mihalic, I. Rodriguez, and D. T. Chiu, Langmuir **19**, 250 (2003).
[26] H. Suzuki and R. Yoneyama, Sens. Actuators B **86**, 242 (2002).
[27] C. Rosslee and N. L. Abbott, Curr. Opin. Colloid Interface Sci. **5**, 81 (2000).